2.5D True-amplitude diffraction-stack redatuming: numerical tests

Francisco Oliveira (UFPA), Matheus F. Pila (PGS), Amélia Novais (Unicamp), Jessé Costa (UFPA) and Jörg Schleicher (Unicamp)

This paper was prepared for presentation at the 11th International Congress of The Brazilian Geophysical Society held in Salvador, Brazil, August 24-28, 2009.

Abstract

The objective of this work is to demonstrate the application of single-stack redatuming. The purpose of this operation is to transform seismic data acquired in a certain measurement level, in order to simulate data as if acquired at another level. Recent theoretical advances allow to perform this transformation for zero-offset data in a single step. The true-amplitude diffraction-stack-type redatuming operator is based on the chaining of diffraction-stack migration and isochron-stack demigration and was developed for zero-offset data. It consists of performing a single weighted stack along adequately chosen stacking lines. In this work, we demonstrate the application of this method to synthetic seismic data for media with two or many flat layers and in models with lateral velocity variations. In the first case the data are generated at and redatumed to flat surfaces, in the second situation both surfaces of aquisition and redatuming have different topographies, and in the third experiment data from a laterally varying medium are redatumed to a flat datum using only velocity information in the top layer. Our examples demonstrate the quality of the redatumed data both kinematically and dynamically.

Introduction

Redatuming is used with the objective to transform seismic data acquired at a certain measurement level to simulate data as if acquired at another level (Wapenaar et al., 1992). The standard way of realizing a redatuming is by downward continuation of seismic time data (Berryhill, 1979, 1984, 1986). The main goal when using redatuming is to improve the data quality. In practice, redatuming is frequently used to remove the interference of topography from the data, simulating the aquisition at a planar datum. However, the general ideas of redatuming are not restricted to the datum being planar. The general redatuming formalism can include topography at both the original aquisition surface and the new datum.

Over the years, many attempts have been made to achieve the goal of determining the seismic data at a new datum. Other contributions to the theory of wave-equation-based redatuming methods include the works of Yilmaz and Lucas (1986), Schuster and Zhou (2006) made a summary about the state of art in redatuming.

As geometrically discussed by Hubral et al. (1996) and mathematically shown by Tygel et al. (1996), redatuming is a true-amplitude configuration transform (particular case), developed from chaining of diffraction stack migration and isochron stack demigration (Pila et al., 2007).

In practice, redatuming is often only employed kinematically, without regard to preserving the amplitudes. However, when we want to use the dynamic information, for instance in a subsequent true-amplitude migration (see, e.g., Schleicher et al., 1993), amplitude preservation is of fundamental importance in the complete processing sequence, including redatuming. In this work, we demonstrate the application of true-amplitude single-stack redatuming to synthetic seismic data for media with two or many flat layers and in models with lateral velocity variations.

Methodology

Redatuming is one of imaging operation that can be described by a chaining of Kirchhoff-type migration and demigration integrals. For this purpose, all that has to be done is to interchange the order of integrations and analytical evaluate the new inner integrals. In this way, many one-step imaging operation of the type of a diffraction stack can be developed (Schleicher et al., 2007).

In this work, we study a 2.5D true-amplitude redatuming, i.e., we study the amplitude behavior when redatuming data. The attribute 2.5D (Bleistein, 1986) indicates that in our experiments we consider 3D wave propagation in a 2D earth model. The velocity is invariable in the y direction and the seismic line is positioned along the x-axis.

The experiment considers the zero-offset situation, with sources and receiver in the same position and equally spaced along the x-axis. We assume that

all point sources and receivers are reproducible, i.e., they possess identical characteristics independently of their actual position.

In the analysis below, the location of the source-receiver positions along the original seismic line on the acquisition surface $\mathcal{Z}_o$ is described by their horizontal coordinate ξ. In other words, the original sources and receivers are located at the points $G = S = (\xi, 0, \mathcal{Z}_o(\xi))$. Correspondingly, the simulated source-receiver positions on the new datum $\mathcal{Z}_r$ are described by their horizontal coordinate η, i.e., they are located at the points $G_r = S_r = (\eta, 0, \mathcal{Z}_r(\eta))$.

We know that for each point (η,τ) in the redatumed section to be constructed, there is a weighted diffraction-stack operation along problem-specific stacking surfaces, the so-called inplanats $t = \mathcal{T}_r(\xi;\eta,\tau)$, that achieves the desired true-amplitude transformation. Accordingly, the simulated data at a new level can be expressed as a single stacking operator with a weight function $W_r(\xi;\eta,\tau)$ acting upon the input data, i.e.,

$$U_r(\eta,\tau) = \frac{1}{\sqrt{2\pi}} \int_A d\xi\, W_r(\xi;\eta,\tau) \, D^{1/2}[U(\xi,t)]|_{t=\mathcal{T}_r(\xi;\eta,\tau)}\,, \quad (1)$$

where $U(\xi,t)$ stands for the input data and $U_r(\eta,\tau)$ represents the redatumed output data. Moreover, A denotes the aperture of the stack, that is, the region over which data are stacked to contribute to the output value at (η,τ). Finally, $D^{1/2}$ is the half-derivative operation which helps to correctly recover the pulse shape of the source wavelet. It can be represented as

$$D^{1/2}[f(t)]| = \mathcal{F}^{-1}\left[|\omega|^{\frac{1}{2}} e^{-i\frac{\pi}{2}sign(\omega)} \mathcal{F}[f(t)]\right], \quad (2)$$

where $\mathcal{F}$ denotes the Fourier transform.

Stacking curve and weight function

The determination of the stacking curve is related to the kinematic properties of the problem. The stacking line connects all point in the input section where a reflection event might have been recorded that would appear in the redatumed section at an output point (η,τ). On the other hand, the weight function is related to the amplitude behaviour. The condition for a true-amplitude weight function is that, asymptotically, the simulated reflections must have the same geometrical-spreading factor that the reflections would have if they were actually acquired on the new datum. As shown by Pila et al. (2007), the resulting true-amplitude weight function does not depend on any reflector property. Thus, it is possible to evaluate it for any point (η,τ) in the redatumed section using only information about the velocity model.

The stacking curve $\mathcal{T}_r$ is determined using two steps:

1) Given a point (η,τ) at the new datum, we must construct the isochron $\mathcal{Z}_{Ir}(x;\eta,\tau)$ in depth. This isochron is defined by all points $M = (x, \mathcal{Z}_{Ir}(x;\eta,\tau))$ in depth for which the sum of traveltimes along the ray segments S_rM and MG_r, which connect the depth point M to the source-receiver pair (S_r, G_r), is equal to the given time τ or, mathematically,

$$T(S_r,M) + T(M,G_r) = 2T(S_r,M) = \tau\,. \quad (3)$$

For the determination of the traveltimes $T(S_r,M)$ and $T(S_r,M)$, a macrovelocity model must be available.

2) In the next stage, we consider the isochron $\mathcal{Z}_{Ir}(x;\eta,\tau)$ as a reflector in an experiment with the input distribution of source-receiver pairs at the original measurement surface $z = \mathcal{Z}_\imath(\xi)$. The resulting traveltime curve can be written as;

$$t = \mathcal{T}_r(\xi;\eta,\tau) = \mathcal{T}_D(\xi;x^*;z^*)\,, \quad (4)$$

where

$$\mathcal{T}_D(\xi;x^*;z^*) = T(S,M^*) + T(M^*,G) = 2T(S,M^*) \quad (5)$$

is the diffraction traveltime curve of the stationary point $M^* = (x^*,z^*)$. For each source-receiver pair at a position ξ, point M^* represents the point on the isochron $z = \mathcal{Z}_{Ir}(x;\eta,\tau)$ where a reflection would occur that would be registered at ξ with a traveltime t. Point M^*, supposed to be unique, has the coordinates $(x^*, z^* = \mathcal{Z}_{Ir}(x^*;\eta,\tau))$, where its horizontal coordinate, $x^* = x^*(\xi;\eta,\tau)$ is obtained from the stationarity condition (Fermat's principle)

$$\frac{\partial}{\partial x}\left[\mathcal{T}_D(\xi;x,z)\right]|_{x=x^*} = 0. \quad (6)$$

Pila et al. (2007) demonstrated that the weight function $W_r(\xi;\eta,\tau)$ can be obtained from a fully analogous analysis to the one presented for migration to zero-offset (MZO) in Tygel et al. (1998). The reason is that both operations belong to the general class of configuration transforms. The arguments and mathematical derivations applied to both situations are the same. The final redatuming weight function for an arbitrary medium, configuration and topography reads,

$$W_r(\xi;\eta,\tau) = \frac{v_{oS}}{v_{iS}} \sqrt{\frac{\sigma_{iS}+\sigma_{iG}}{\sigma_{oS}+\sigma_{oG}}} \frac{\overline{\mathcal{L}}_{iS}\overline{\mathcal{L}}_{iG}}{\overline{\mathcal{L}}_{oS}\overline{\mathcal{L}}_{oG}} \left(\frac{\cos\theta_s}{\overline{\mathcal{L}}_{iS}^2} + \frac{\cos\theta_G}{\overline{\mathcal{L}}_{iG}^2}\right) \frac{1}{\cos\phi} \sqrt{\frac{\cos\theta_{oR}}{v_R^3}} \frac{\exp\{i\pi[1-sgn(K_i-Ko)]/4\}}{\sqrt{2|K_i-Ko|}}, \quad (7)$$

where v_{iS}, v_{oS}, v_R are the velocities at the sources on the input, output datums and at point M, re-

spectively. Also, σ_{iS}, σ_{iG} are the so-called optical lengths of ray segments MS_i and MG_i, respectively, i.e., the integral of squared velocity in traveltime along the ray. Analogously, σ_{oS}, σ_{oG}, represent these factors along segments MS_o and MG_o, respectively. These factors represent the out-of-plane geometrical-spreading factors.

The in-plane components of the geometrical spreading are given by $\overline{\mathcal{L}}_{iS}$ and $\overline{\mathcal{L}}_{iG}$, along segments MS_i and MG_i, and $\overline{\mathcal{L}}_{oS}$ and $\overline{\mathcal{L}}_{oG}$, along segmentes MS_o and MG_o, respectively. Moreover, symbols θ_{iS} and θ_{iG} represent the angles that the rays M_{Si} and M_{Gi} make with the surface normal at S_i and G_i, respectively, and ϕ is the surface dip angle at S_i. In addition, θ_{oR} is the reflection angle at M in output configuration Finally, K_i and K_o are the curvatures of the input and output isochrons, respectively. For the zero-offset configuration, Pila et al. (2007) simplified expression (7) to

$$W_r(\xi;\eta,\tau) = \frac{v_{oS}}{v_{iS}}\sqrt{2\frac{\sigma_{iS}}{\sigma_{oS}}}\frac{\cos\theta_s}{\cos\phi}\frac{1}{v_R^{3/2}\overline{\mathcal{L}}_{oS}^2}\frac{\exp\{i\pi k/2\}}{\sqrt{K_i-K_o}}\,. \tag{8}$$

Homogeneous medium without topography

For simple velocity models, the stacking curve (4) and weight function (7) can be further simplified. For example, for a homogeneous medium with a flat surface and a flat datum, i.e., $z_i(x)=0$ and $z_r(x)=z_r$, the geometry reduces to the one depicted in Figure 1.

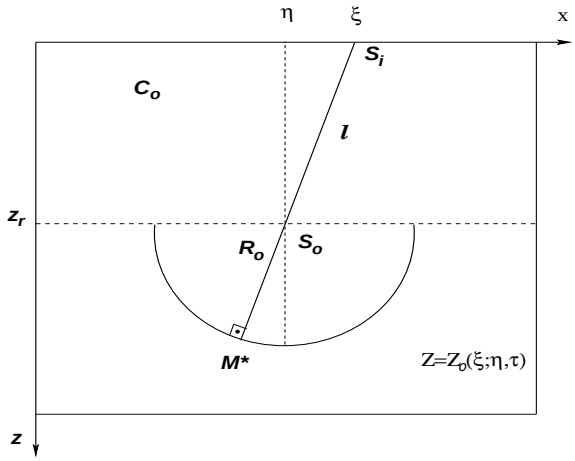

Figure 1: The unique reflection from an input source-receiver pair to the isochron $z = Z_o(\xi;\eta,\tau)$ crosses the center of the semicircular isochron.

The stacking curve and the weight function for this case were derived by Pila et al. (2007), resulting in

$$\mathcal{T}_r(\xi;\eta,\tau) = \frac{2}{v_o}(R_o+\ell) = \tau + 2\frac{\ell}{v_o} \tag{9}$$

and

$$W_r(\xi;\eta,\tau) = \sqrt{\frac{2}{v_o}}\left(\frac{R_o+\ell}{R_o}\right)\frac{z_r}{\ell^{3/2}}. \tag{10}$$

Homogeneous medium with topography

Pila et al. (2007) have also shown how the stacking line and weight function must be modified if topography is present at the acquisition surface $z_i = z_i(\xi)$ and at the datum $z_r = z_r(\eta)$. The stacking curve (4) is still valid, with ℓ denoting the distance between S_i and S_o, and in the weight function (8), the factor z_r needs to be replaced by

$$z_r \rightarrow [z_r(\eta) - z_i(\xi) - (\xi-\eta)z_i'(\xi)]\,. \tag{11}$$

Numerical experiments

The validity of the theory was confirmed by Pila et al. (2007) by a numerical test in homogeneous models. In this work, we extend the validity of the redatuming operation to slightly more complicated models.

First model

In the first synthetic experiment, we apply constant-velocity redatuming to a horizontally layered model with five horizontal layers with acoustic wave velocitys of 1500 m/s, 1800 m/s, 2500 m/s, 3300 m/s, and 4000 m/s. Figure 2 shows the geometry of the reflectors together with the ray family of the chosen zero-offset configuration. The source-receiver pairs

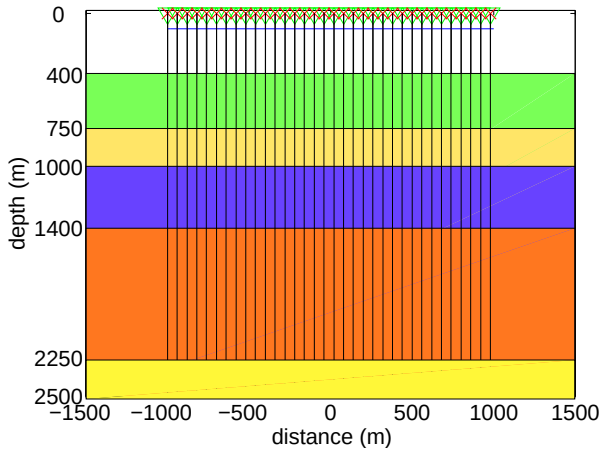

Figure 2: Model for the first numerical experiment: A zero- offset experiment was simulated at z = 0 above set of plain reflectors. Also shown is the datum level (blue line) at $z = 100$ m.

are positioned at at $z = 0$ m at every 20 m between $\xi = -1000$ m and $\xi = 1000$ m. Also show in Figure 2 is the new datum level at $z = 100$ m (blue line). We generated the synthetic data using Kirchhoff modeling in the RMS velocity model (see Figure 3). These data have then been used as input for redatuming operation (1), with stacking line (9) and weight function (10) using the correct RMS velocity model. The output configuration also consists of source-receiver pairs at every 20 m between $\eta = -1000$ m and $\eta = 1000$ m. The resulting redatumed data are depicted in Figure 4. For comparison, Figure 5 shows

the ideal result of this redatuming operation, i.e., the section obtained by direct Kirchhoff modeling at the datum level. Comparing Figures 4 and 5, we recognize that the kinematic transformation was very good. The structure of the redatumed reflection data looks identical to the one of the modeled data. Also, the amplitudes of the five events are correctly recovered. Some operator noise is visible after the events. For

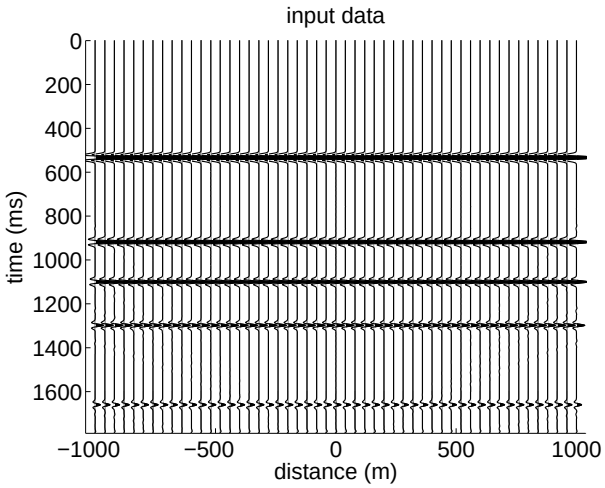

Figure 3: Modeled seismic zero-offset section.

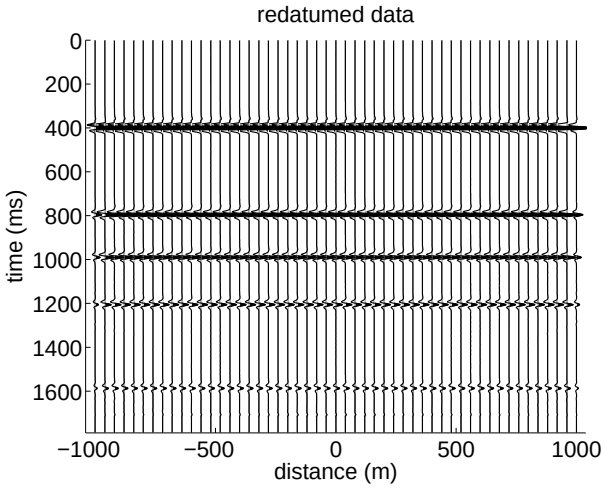

Figure 4: Section resulting from redatuming operation (1) to $z = 100$ m.

a more detailed appreciation of the quality of the redatumed data, Figure 6 shows a comparison of the central traces of Figures 4 and 5. We see that the five events are well recovered.

Second model

In the second synthetic test, the acquisition surface and datum have different sinoidal topographies (see Figure 7). The model consists of two homogeneous and isotropic flat layers with acoustic wave velocitys of 1500 m/s and 1800 m/s. Figure 7 shows the geometry of the reflector together with the ray family of the chosen zero-offset configuration. The source-receiver pairs are positioned at every 20 m between $\xi = -1000$ m and $\xi = 1000$ m. Also show in Figure 7

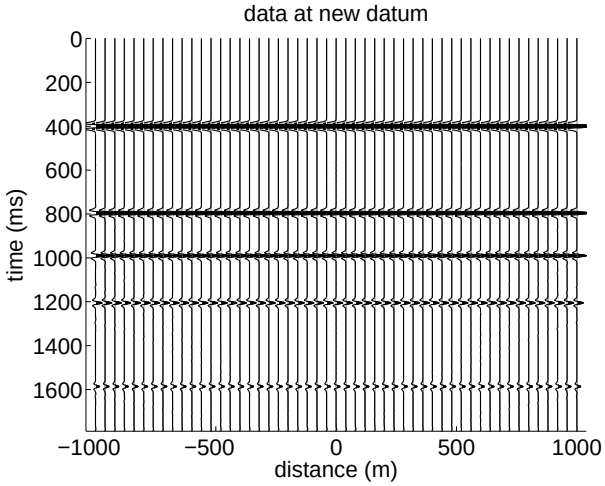

Figure 5: Section resulting from Kirchhoff modeling at $z = 100$ m.

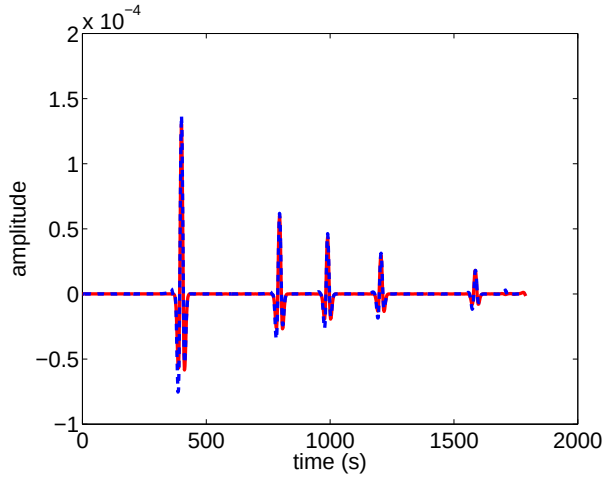

Figure 6: Comparison of the central traces of Figures 4 and 5. Notice the good coincidence between the redatumed (dashed line) and modeled (continuous line) traces.

the new datum surface at $z = z_r(\eta)$ (blue line).

The synthetic Kirchhoff data for the model in Figure 7 are depicted in Figure 8. They have then been used as input for single-stack redatuming. The output configuration also consists of source-receiver pairs at every 20 m between $\eta = -1000$ m and $\eta = 1000$ m. The resulting data are depicted in Figure 9. For comparison, Figure 10 shows the ideal result of this redatuming operation. The section in Figure 10 was obtained by direct Kirchhoff modeling at the datum level. Comparing Figures 9 and 10, we recognize that the kinematic transformation was very good. The structure of the redatumed reflection data looks identical to the one of the modeled data. Some operator noise is visible after the event. For a more quantitative comparison, Figure 11 compares the central trace of modeled an redatumed sections in Figures 8 and 9. We notice the almost perfect coincidence between the redatumed (dashed line) and modeled (continuous line)

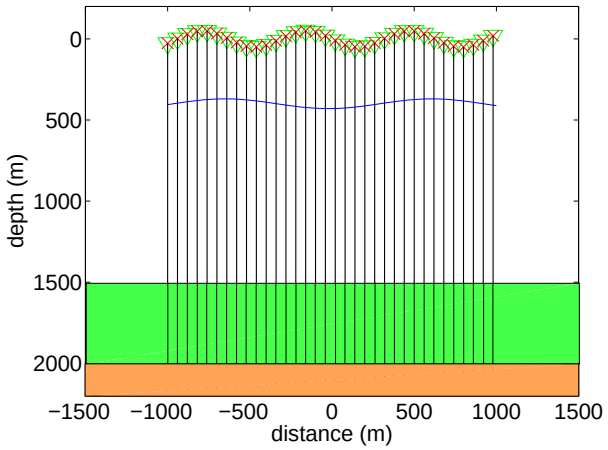

Figure 7: Model for the second numerical experiment: A zero-offset experiment was simulated at $z_i = z_i(\xi)$ above a flat reflector. Also shown is the datum level (dotted line) at $z_r = z_r(\eta)$ m.

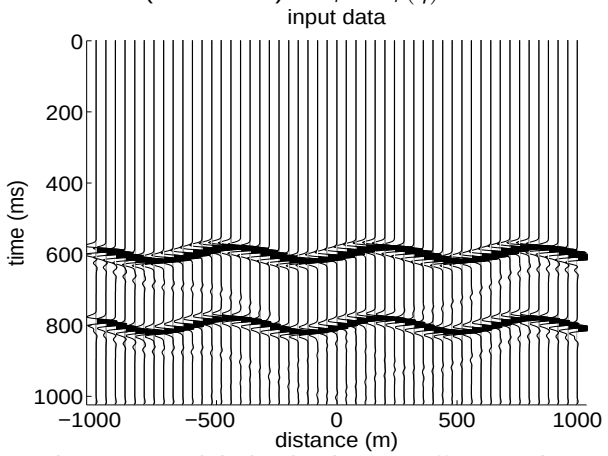

Figure 8: Modeled seismic zero-offset section.

traces.

Model with lateral velocity variations

The third model consists of four smoothly curved interfaces separating homogeneous layers with velocities 1508 m/s, 1581 m/s, 1690 m/s, 1826 m/s, and 2000 m/s (Figure 12). We modeled synthetic zero-offset data by Gaussian beams at the planar surface with source-receiver pairs at every 50 m between $\xi = 0$ m and $\xi = 4000$ m (Figure 13). Then, we redatumed these data to a depth of $z_r = 100$ m (Figure 14) using the velocity of the topmost layer and compared them to data modeled at the datum level (Figure 15). The two sections look almost identical.

Conclusions

The redatuming operation can be thought of as being composed of a true-amplitude diffraction-stack migration and true-amplitude isochron-stack demigration, as described in the unified approach to seismic reflection imaging (Hubral et al., 1996; Tygel et al., 1996). Based on this observation, Pila et al. (2007) derived analytic expressions for the stacking line and

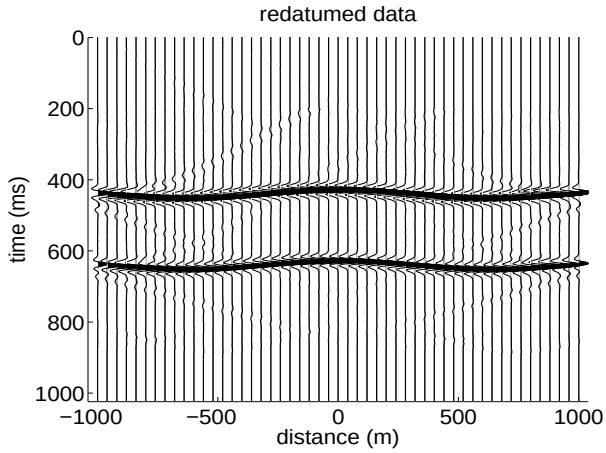

Figure 9: Section resulting from redatuming to $z_r(\eta)$.

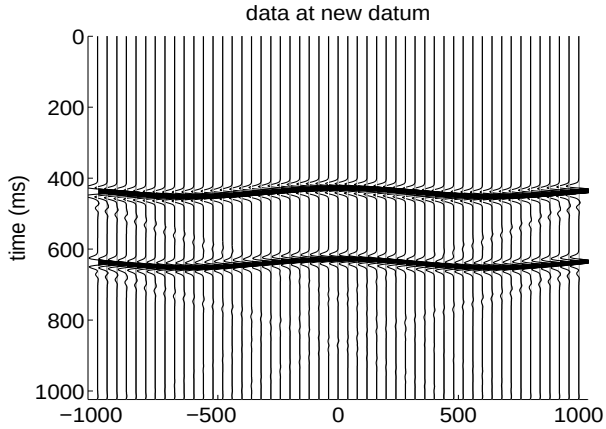

Figure 10: Section resulting from Kirchhoff modeling at $z_r(\eta)$.

weight function of a single-stack redatuming.

In this work, we have applied the redatuming operator of Pila et al. (2007) to different synthetic data of models with two or more layers and in models with lateral velocity variations. In these experiments, we have seen that seismic data acquired at the measurement surface were repositioned correctly to a new level, preserving attributes as amplitude and phase. The topography did not present a restriction to the application of the method.

Further investigations are being carried to test the potential of the redatuming operator for applications in others models with lateral velocity variations.

Acknowledgment

This work has been partially supported by the National Council of Scientific and Technological Development (CNPq), Brazil, as well as Petrobras and the sponsors of the Wave Inversion Technology (WIT) Consortium, Germany.

References

Berryhill, J. R., 1979, Wave-equation datuming: Geophysics, 44, 1329–1344.

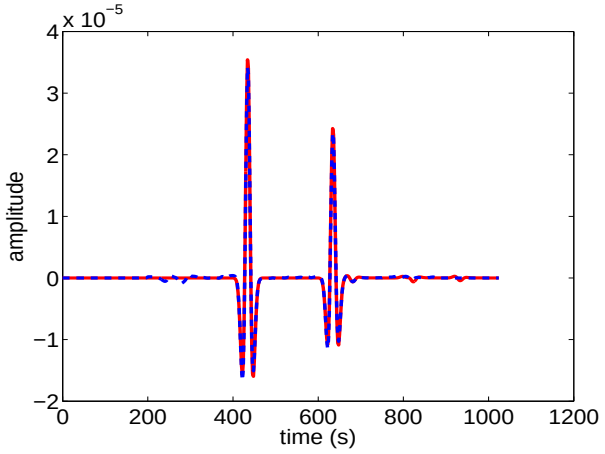

Figure 11: Comparison of the central traces of Figures 9 and 10. Notice the good coincidence between the redatumed (dashed line) and modeled (continuous line) traces.

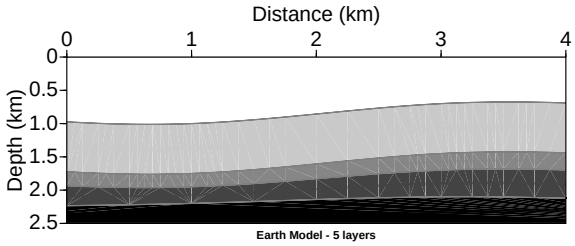

Figure 12: Laterally inhomogeneous model for the third synthetic experiment.

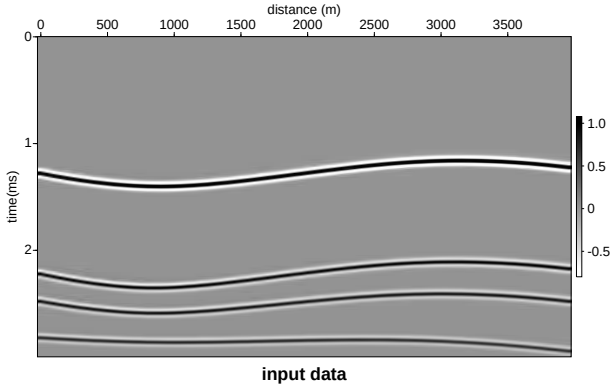

Figure 13: Modeled seismic zero-offset section.

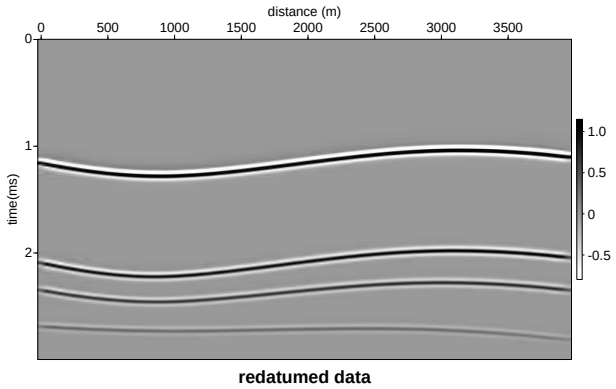

Figure 14: Section resulting from redatuming to $z = 100\ m$

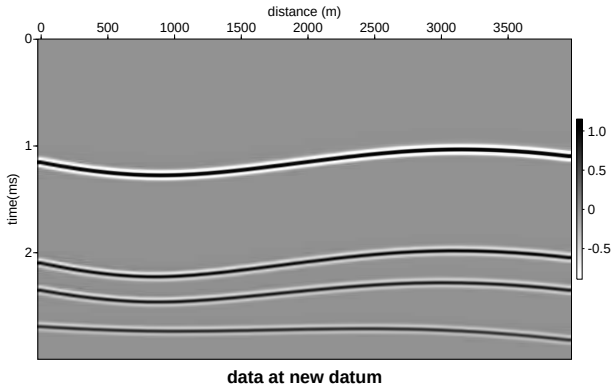

Figure 15: Section resulting from modeling at $z = 100\ m$

Berryhill, J. R., 1984, Wave equation datuming before stack: Geophysics, 49, 2064–2067.

Berryhill, J. R., 1986, Submarine canyons–velocity replacement by wave equation datuming before stack: Geophysics, 51, 1572–1579.

Bleistein, N., 1986, Two-and-one-half dimensional in-plane wave propagation: Geophysical Prospecting, 34, 686–703.

Hubral, P., J. Schleicher, and M. Tygel, 1996, A unified approach to 3–D seismic reflection imaging – Part I: Basic concepts: Geophysics, 61, 742–758.

Pila, M., Schleicher, J., A. Novais, 2007, True-amplitude diffraction-stack redatuming:Tenth International Congress of the Brazilian Geophysical Socity.

Schleicher, J., Tygel M., and P. Hubral, 1993, 3–D true–amplitude finite–offset migration: Geophysics, 58,1112–1126.

Schleicher, J., Tygel M., and P. Hubral, 2007, Seismic true–amplitude imaging: SEG Monograph.

Schuster, G. T. and M. Zhou, 2006, A theoretical overview of model based and correlation based redatuming methods: Geophysics, 71,103–110.

Tygel, M., J. Schleicher, and Hubral, P. 1994, Pulse distortion in depth migration: Geophysics, 59, 1561–1569.

Tygel, M., J. Schleicher, and P. Hubral, 1996, A unified approach to 3-D seismic reflection imaging–Part II: Theory: Geophysics, 61, 759–775.

Tygel, M., J. Schleicher, P. Hubral, and L. T. Santos, 1998, 2.5D true-amplitude Kirchhoff migration to zero offset in laterally inhomogeneous media: Geophysics, 63, 557–573.

Wapenaar, C. P. A., H. L. H. Cox, and A. J. Berkhout, 1992, Elastic Redatuming of multicomponent seismic data: Geophysical Prospecting, 49, 1239–1248.

Yilmaz, O. and D. Lucas, 1986, Prestack layer replacement: Geophysics, 51, 1355–1369.